Macromolecules

ARTICLE

pubs.acs.org/Macromolecules

Double-Gyroid Network Morphology in Tapered Diblock Copolymers

Raghunath Roy,[†] Jong Keun Park,[†] Wen-Shiue Young, Sarah E. Mastroianni, Maëva S. Tureau, and Thomas H. Epps, III*

Department of Chemical Engineering, University of Delaware, Newark, Delaware 19716, United States

Supporting Information

ABSTRACT: We report the formation of a double-gyroid network morphology in normal-tapered poly(isoprene-*b*-isoprene/styrene-*b*-styrene) [P(I−IS−S)] and inverse-tapered poly(isoprene-*b*-styrene/isoprene-*b*-styrene) [P(I−SI−S)] diblock copolymers. Our tapered diblock copolymers with overall poly(styrene) volume fractions of 0.65 (normal-tapered) and 0.67 (inverse-tapered), and tapered regions comprising 30 vol % of the total polymer, were shown to self-assemble into the double-gyroid network morphology through a combination of small-angle X-ray scattering (SAXS) and transmission electron microscopy (TEM). The block copolymers were synthesized by anionic polymerization, where the tapered region between the pure poly(isoprene) and poly(styrene) blocks was generated using a semibatch feed with programmed syringe pumps. The overall composition of these tapered copolymers lies within the expected network-forming region for conventional poly(isoprene-*b*-styrene) [P(I−S)] diblock copolymers. Dynamic mechanical analysis (DMA) clearly demonstrated that the order−disorder transition temperatures (T_{ODT}'s) of the network-forming tapered block copolymers were depressed when compared to the T_{ODT} of their nontapered counterpart, with the P(I−SI−S) showing the greater drop in T_{ODT}. These results indicate that it is possible to manipulate the copolymer composition profile between blocks in a diblock copolymer, allowing significant control over the T_{ODT}, while maintaining the ability to form complex network structures.

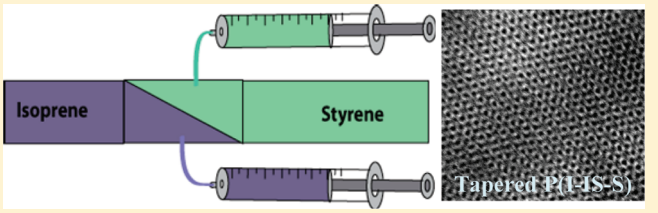

I. INTRODUCTION

Block copolymers are an exciting class of materials due to their ability to self-assemble into periodic nanoscale structures.[1−3] The tendency for diblock copolymers to phase separate into various nanostructures can generally be characterized by the parameters $\chi_{AB}N$ and f_A. Here, χ_{AB} is the Flory−Huggins interaction parameter between A and B segments, N is the overall degree of polymerization, and f_A is the volume fraction of block A. According to the poly(isoprene-*b*-styrene) P(I−S) phase diagram,[4] a variety of ordered structures such as body-centered cubic spheres, hexagonally packed cylinders, double-gyroid, and lamellae can be formed in the P(I−S) system when the product $\chi_{AB}N$ is greater than a critical value, $(\chi_{AB}N)_{ODT}$ (ODT = order−disorder transition).

Literature reports have shown that three-dimensional network morphologies, such as the double gyroid with $Ia\bar{3}d$ symmetry,[5−8] may offer superior mechanical attributes relative to their one- and two-dimensional counterparts (e.g., lamellae and cylinders).[9] These networks are ideally suited for membrane and ion-conducting applications due to their well-defined diffusion pathways.[8] Furthermore, block copolymer network structures offer opportunities to improve transport in organic conducting systems, such as organic solar cells by facilitating the separation and extraction of free charges due to their cocontinuity and large internal interfacial area, along with controlled domain sizes on the order of exciton diffusion lengths.[8,10,11] Thus, a detailed understanding of the influence of interfacial structure on gyroid-forming materials is warranted. Although limited studies have commented on the formation of network structures in interfacially manipulated block copolymers, the ability to form these materials as a function of taper compositions (and the composition effect on T_{ODT}) has not been explored experimentally.[12,13]

For the majority of AB diblock copolymers, the composition profile along the polymer backbone changes abruptly at the junction between A and B copolymer segments. This standard composition profile in block copolymers can be easily modified by introducing a transition region between the pure A and B blocks that tapers from A to B units (referred to as normal-tapered) or from B to A units (referred to as inverse-tapered).[14−18] AB diblock copolymers containing a random A/B transition region also can be considered a subset of tapered block copolymers for smaller random A/B region volume fractions.[13]

Although they are not the focus of this investigation, a brief comment should be made regarding gradient copolymers to distinguish them from tapered block copolymers in regards to the length of the compositional transition region. Gradient copolymers employ a change in composition from mostly A-monomer to mostly B-monomer along much or all of the copolymer chain length while tapered block copolymers have a distinct gradient region along only part of the polymer chain.[16,19−22]

Received: November 12, 2010
Revised: March 23, 2011
Published: May 02, 2011

Furthermore, in melt-state gradient copolymers, structural evidence of phase segregation has been limited to lamellar morphologies as theoretically suggested by Jiang et al.[21]

From a synthetic point of view, interfacial modification through tapering constitutes an additional design parameter that permits both further manipulation of interfacial structure and greater understanding of that interfacial structure on bulk copolymer self-assembly. In previous literature, tapered block copolymers were prepared by taking advantage of the greater reactivity ratio of isoprene versus styrene in hydrocarbon solutions of an alkyllithium, which leads to the propagating polymer chain initially being rich in isoprene and then gradually tapering to chain segments rich in styrene.[17,23] For example, Hodrokoukes et al. synthesized a normal-tapered poly(isoprene-*b*-isoprene/styrene-*b*-styrene) by starting the reaction with the addition of isoprene to *sec*-butyllithium (*s*-BuLi), followed by the addition of a mixture of the isoprene and styrene monomers, and finally the addition of styrene. To synthesize an inverse-tapered poly(isoprene-*b*-styrene/isoprene-*b*-styrene), the reaction was started with the addition of styrene, followed by a mixture of the isoprene and styrene monomers, and finally the addition of isoprene.

Previously, our group demonstrated the incorporation of tapered regions between pure poly(isoprene) and poly(styrene) blocks using a combination of a semibatch feed and anionic polymerization techniques.[18] Automated syringe pumps were employed to inject predetermined amounts of monomers into a reactor at varying flow rates to achieve precise control over the desired composition of the tapered segment. The incorporation of tapered regions between pure blocks has been shown to increase block miscibility, which is manifested in the widening of the interphase region in self-assembled systems.[17]

Related to the current investigation, the work by Hashimoto and co-workers to create tapered diblock copolymers deserves attention.[12,14] The authors copolymerized a mixture of styrene and isoprene monomers in the presence of a trace amount of tetrahydrofuran (THF, ca. 1 vol % of the polymerization solvent) using benzene as the polymerization solvent. The THF was added with the intent of increasing mixing between the two monomers in the copolymer chain, thus reducing the "blockiness" of the sequence distribution. On the basis of TEM results, the morphology of the final polymer (styrene 42 vol % and M_n = 1.06×10^5 g/mol) was suggestive of a network structure. While pyrolysis gas chromatography and ^{1}H NMR indicated mixing of isoprene and styrene monomers along the block copolymer chain, the authors were unclear about whether the monomer distribution led to a tapered or random copolymer.[14] Further, the authors indicated that the copolymerization exhibited a tenuous reddish-yellow color throughout the polymerization reaction, hinting that controlled tapering may not have been achieved.[14]

While tapered block copolymers afford the ability to manipulate the interfacial composition profile, to the authors' knowledge, no systematic attempts to generate network-forming tapered block copolymers have been reported in the literature. Additionally, the majority of previous reports on tapered block copolymers have focused on polymers with symmetric compositions, which have led to the formation of self-assembled lamellar morphologies,[15,17,18,24] with a notable exception.[24] By introducing a tapered middle region which allows controlled interfacial width and tunability of the order−disorder transition temperature (T_{ODT}), we report on the self-assembly and thermal characterization of double-gyroid network-forming tapered block copolymers, using a poly(isoprene-*b*-styrene) [P(I-S)] base system.

II. EXPERIMENTAL SECTION

Synthesis of Tapered Diblock Copolymers. The semibatch synthesis of normal-tapered and inverse-tapered diblock copolymers was achieved following a previously published procedure.[18] In summary, *sec*-butyllithium was used as the initiator for the sequential living anionic polymerization of a poly(isoprene) block, followed by a tapered region of isoprene and styrene, and finally a poly(styrene) block. The tapered region was targeted to 30% of the total copolymer volume. During the tapering step of the polymerization, the required amounts of monomers were injected into the reactor using programmable syringe pumps at predetermined flow rates over 5 h to obtain the desired linear composition profile (from pure A to pure B for the normal-tapered region and from pure B to pure A for the inverse-tapered region). Following completion of the PS block, the living P(I−IS−S) and P(I−SI−S) were end-capped with an ethylene oxide (EO) repeat unit, and the polymerizations were terminated with degassed methanolic HCl to obtain P(I−IS−S)−OH and P(I−SI−S)−OH, respectively. A nontapered P(I−S)−OH diblock copolymer was synthesized in similar fashion except for the absence of the tapering step. The hydroxyl end group on all three copolymers can be utilized in further polymerization or functionalization steps.[25−27]

Chemical Characterization. The number-average molecular weights and polydispersity indices of the nontapered, normal-tapered, and inverse-tapered block copolymers were determined by gel permeation chromatography (GPC) using a Viscoteck 270max instrument fitted with Waters Styragel HR1 and HR4 columns in series, operated with THF as the mobile phase, and calibrated with poly(styrene) standards (GPC traces can be found in the Supporting Information). Details on the taper composition profile can be found elsewhere.[18] The overall polymer compositions for P(I−S)−OH, P(I−IS−S)−OH, and P(I−SI−S)−OH were calculated from integrated ^{1}H NMR peak intensities obtained using a Bruker AV-400, which were converted to volume fractions using homopolymer densities at 140 °C (ρ_{PI} = 0.83 g/mL, ρ_{PS} = 0.97 g/mL).[28]

Small-Angle X-ray Scattering (SAXS). To investigate the morphology of the block copolymers, synchrotron SAXS experiments were conducted on the DND-CAT of the Advanced Photon Source (APS) at Argonne National Laboratory and on the X27C beamline of the National Synchrotron Light Source (NSLS) at Brookhaven National Laboratory. In this work, the SAXS patterns obtained at the APS and NSLS facilities are referred to as "APS-SAXS" and "NSLS-SAXS" data, respectively. The APS-SAXS experiments were performed using an incident beam wavelength, λ = 0.729 Å and a sample-to-detector distance of 4.035 m, and the NSLS-SAXS experiments were conducted using an incident beam wavelength, λ = 1.371 Å, and a sample-to-detector distance of 1.803 m. Both APS and NSLS data were acquired on a Mar CCD area detector. SAXS data were plotted as azimuthally averaged scattering intensity versus scattering vector modulus, $q = |\mathbf{q}| = 4\pi\lambda^{-1} \sin(\theta/2)$, where θ is the scattering angle. The following annealing protocol was employed during data acquisition to investigate any morphological variations as a function of annealing temperature: (i) The temperature was initially ramped to 150 °C and held for 25 min, (ii) further increased to 200 °C and held for 20 min, and finally (iii) cooled to room temperature (∼30 °C). SAXS data were acquired during each step of the annealing process.

Transmission Electron Microscopy (TEM). Transmission electron microscopy (TEM) was conducted using a JEOL JEM-2000FX microscope operating at 200 kV. The following annealing protocol was employed for the normal-tapered and inverse-tapered block copolymers: (i) the temperature was initially ramped to 180 °C and held for 1 h, (ii) decreased to 150 °C and held for 8 h, (iii) decreased to 100 °C and held for 2 h, and finally (iv) cooled to room temperature (∼30 °C). For the nontapered block copolymer: (i) the temperature was initially

ramped to 220 °C and held for 1 h, (ii) decreased to 200 °C and held for 1 h, (iii) decreased to 150 °C and held for 5 h, and finally (iv) cooled to room temperature (∼30 °C). The specimens were then cut at −70 °C on a Leica Reichart Ultracut cryo-microtome using a Diatome diamond knife. The sliced samples were placed on 400 mesh copper grids and stained with OsO_4 vapor for ∼10 min, which preferentially stained the I-domains of the copolymer.

Dynamic Mechanical Analysis (DMA). Powder samples were hot-pressed into ∼1 mm thickness disks at 110 °C for 20 min. Dynamic mechanical experiments were conducted on a TA Instruments ARES-G2 strain-controlled rheometer in a 25 mm parallel plate geometry under a nitrogen atmosphere. Isochronal storage (G') and loss (G'') modulus measurements were collected on heating and cooling at 1 °C/min at a strain amplitude of 1% and a frequency of 0.5 Hz. Temperature sweeps on the tapered block copolymers were performed between 110 °C and several degrees above order−disorder transition temperatures (T_{ODT}) for two cycles. Temperature sweeps on the nontapered block copolymer were performed as follows: (first heating) the sample was heated from 110 to 220 °C and held for 1 h; (second heating) the sample was heated from 110 °C to several degrees above T_{ODT}. The complete DMA profile for P(I−S)−OH can be found in the Supporting Information. The T_{ODT} values obtained on second heating are reported for all samples.

III. RESULTS

The tapered volume percents, number-average molecular weights (M_n), polydispersity indices (PDI = M_w/M_n), and isoprene volume fractions (f_I) of the block copolymers are reported in Table 1. Isoprene volume fractions of P(I−IS−S)−OH (f_I = 0.35), P(I−SI−S)−OH (f_I = 0.33), and P(I−S)−OH (f_I = 0.36) were deliberately targeted because nontapered poly(isoprene-*b*-styrene) diblock copolymers with the comparable compositions and molecular weights were previously shown to exhibit a bicontinuous gyroid morphology.[5,6] Thus, the effect of the tapered interface on the overall morphological behavior may be studied.

Table 1. Molecular Characteristics of the Block Copolymers

polymer	tapered (vol %)	M_n[a] (g/mol)	volume fraction (f_I)	PDI (M_w/M_n)[a]
P(I−IS−S)−OH	30	33 500	0.35	1.08
P(I−SI−S)−OH	30	38 900	0.33	1.10
P(I−S)−OH[b]	0	38 700	0.36	1.09

[a] Number-average molecular weights (M_n) and polydispersity indices (PDI) were determined using gel permeation chromatography with poly(styrene) standards. [b] The P(I−S)−OH block copolymer contained 1.5 ± 1% of PI homopolymer; however, we do not expect this small amount of homopolymer to significantly affect the morphology at constant composition (i.e., if the homopolymer fraction was replaced by block copolymer at constant composition).[27,29]

Figure 1a shows APS-SAXS profile for the normal-tapered P(I−IS−S)−OH obtained at 30 °C after thermal annealing. We note that the first and second reflections in the SAXS data are strong, and all other peaks have relatively low intensities as shown experimentally and theoretically by Hajduk et al. for the double-gyroid morphology.[6] Additionally, the intensity ratio between the first and second peaks is ∼10:1, similar to that previously reported for the bicontinuous double-gyroid morphology.[30] Furthermore, examination of the SAXS profile reveals that the diffraction pattern is consistent with relative peak assignments of $q/q^* = \sqrt{6}, \sqrt{8}, \sqrt{14}, \sqrt{20}, \sqrt{22}, \sqrt{24}, \sqrt{26}, \sqrt{30}, \sqrt{32}, \sqrt{38}, \sqrt{42}, \sqrt{46}$, and $\sqrt{50}$. The principal peak corresponds to $q^*\sqrt{6}$, where $q^* = q_{112}$, which supports a double-gyroid assignment.[5,31] Though the expected scattering peaks at $q/q^* = \sqrt{16}, \sqrt{34}, \sqrt{40}$, and $\sqrt{48}$ are not distinguishable in the SAXS data, their expected positions have been indicated by dashed arrows in Figure 1a. From the primary peak position, the domain spacing was 54 nm (using $d_{112} = 2\pi/q^*$).

Parts b and c of Figure 1 show NSLS-SAXS profiles for the inverse-tapered P(I−SI−S)−OH and the nontapered P(I−S)−OH, respectively, obtained at 30 °C after thermal annealing. Interestingly, the overall SAXS patterns for P(I−IS−S)−OH, and P(I−SI−S)−OH are very similar to that for P(I−S)−OH, which indicates the incorporation of tapered regions up to 30% of the total copolymer volume did not extinguish the double-gyroid morphology. We also note that the scattering intensities around $\sqrt{38}$ and $\sqrt{50}$ in the P(I−IS−S)−OH and P(I−SI−S)−OH are relatively low compared to those in the P(I−S)−OH, which could be ascribed to changes in scattering behavior due to the slight differences in composition and density profiles of the tapered interfaces. From the primary peak positions, the domain spacings were 64 and 62 nm for the P(I−SI−S)−OH and P(I−S)−OH, respectively.

TEM analysis provides further support for the $Ia\bar{3}d$ space group indexing of the SAXS profiles. TEM micrographs of P(I−IS−S)−OH (Figure 2a), P(I−SI−S)−OH (Figure 2c), and P(I−S)−OH (Figure 2d) show the distinctive "wagon-wheel" pattern indicative of the double-gyroid morphology,[7,32,33]

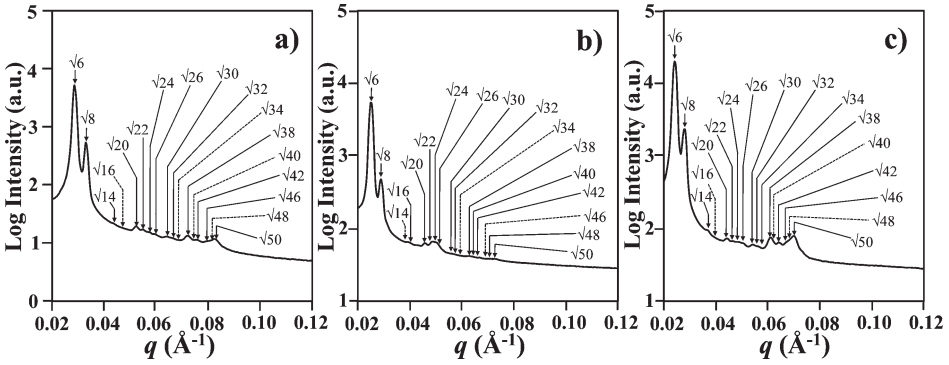

Figure 1. Synchrotron small-angle X-ray scattering (SAXS) data at 30 °C for (a) P(I−IS−S)−OH, (b) P(I−SI−S)−OH, and (c) P(I−S)−OH. In all SAXS profiles, peaks are indexed according to the $Ia\bar{3}d$ space group, characteristic of the double-gyroid morphology; solid (clearly observed) and dashed (expected) lines indicate the peak locations.

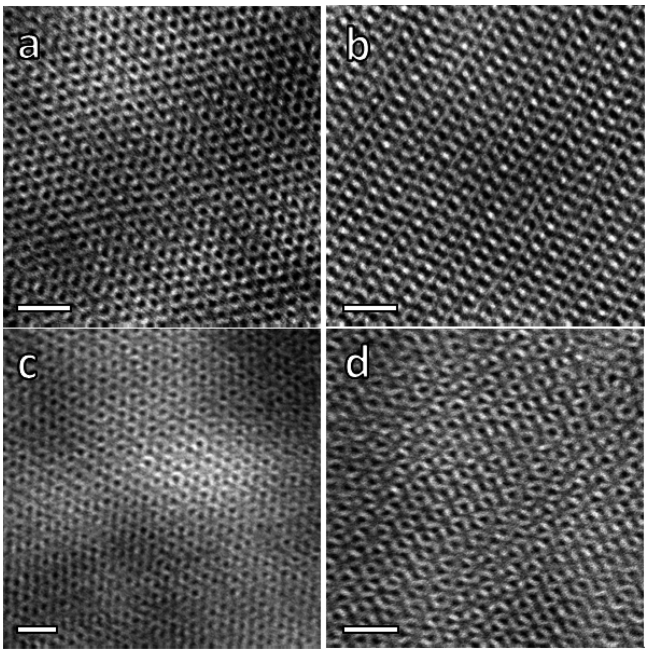

Figure 2. TEM micrographs for P(I−IS−S)−OH (a and b), P(I−SI−S)−OH (c), and P(I−S)−OH (d) representative of the double-gyroid network morphology. The TEM images in (a, c, and d) depict the "wagon-wheel pattern" previously reported in the literature,[7,32,33] characteristic of the [111] double-gyroid projection. The TEM image for P(I−IS−S)−OH (b) obtained from the same specimen displays an orientation that closely resembles the [125] double-gyroid projection. Scale bars represent 100 nm.

characteristic of the [111] projection. The TEM micrograph of P(I−IS−S)−OH in Figure 2b shows a different projection from the same specimen that closely resembles the [125] projection for double-gyroid morphology.[5]

Dynamic mechanical analysis (DMA) experiments were performed to determine the T_{ODT}'s of the tapered and nontapered block copolymers. Figure 3 shows the isochronal storage modulus (G') of all three gyroid-forming materials as a function of temperature (plotted as log G' vs temperature). The sudden drop in G' (marked by arrows) is indicative of the T_{ODT} and correspond to the T_{ODT}'s of P(I−IS−S)−OH, P(I−SI−S)−OH, and P(I−S)−OH, which are 195, 174, and 282 °C, respectively.[34] Analysis of the T_{ODT} data for the tapered and nontapered block copolymers clearly suggests that the introduction of the tapering between blocks (30 vol %) significantly influenced segmental interactions at the interface in the self-assembled network structures, and this influence was manifested by measurable decreases in order−disorder transition temperatures of the tapered materials when compared to a similar nontapered specimen.

IV. DISCUSSION

Our approach for creating tapered regions using automated syringe pumps allows us to maintain precise control over the desired length and composition of the tapered segments. In addition to using ^{1}H NMR and GPC to monitor our tapers,[18] progress of tapering was visually confirmed by monitoring the color change of the reaction mixture throughout the copolymerization. For example, the normal tapering polymerization (from pure isoprene segments to pure styrene segments) exhibited a gradual color change from colorless to orange as the

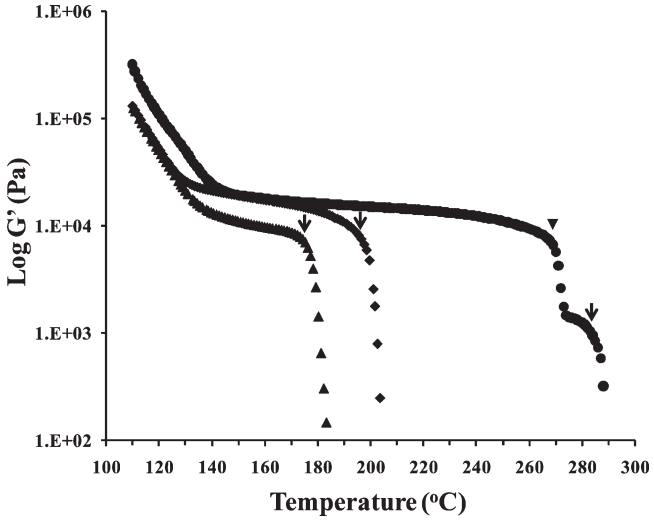

Figure 3. Isochronal storage modulus (G') vs temperature for P(I−IS−S)−OH (♦), P(I−SI−S)−OH (▲), and P(I−S)−OH (●). A frequency of 0.5 Hz and a heating rate of 1 °C/min were used for all samples. The order−disorder temperatures (T_{ODT}'s) are indicated by arrows. We note that the P(I−S)−OH sample showed an order−order transition (OOT), indicated by the ▼ prior to T_{ODT}. We suspect that this OOT delineates a transition between the gyroid and cylindrical phases; however, the details are not explored in this work.

tapering was achieved. On the other hand, during the inverse tapering polymerization (from pure styrene segments to pure isoprene segments), the solution color changed gradually from orange to colorless as tapering proceeded.[18]

Both SAXS and TEM results are consistent with double-gyroid assignments for the normal-tapered, inverse-tapered, and nontapered block copolymers. Förster et al.[5] and Hajduk et al.[6] prepared nontapered poly(isoprene-*b*-styrene) diblock copolymers with comparable composition and molecular weight (M_n) to our tapered copolymers and showed their nontapered morphology to be double gyroid. Thus, it could be inferred that modification of the interface by introducing a tapered region (30 vol % of the overall copolymer) did not significantly influence the overall morphological behavior. It is also worth noting that the terminal hydroxyl groups on the tapered and nontapered block copolymers did not significantly affect the phase behavior near the network phase window most likely due to the small volume fraction of hydroxyl groups in the overall polymer.[35,36] We suspect that the −OH groups may affect T_{ODT} relative to non-hydroxyl-terminated materials; however, given that all of our materials have the same terminus, we do not expect these end groups to influence our reported trends in thermal behavior (see below).

According to mean-field theories, the order−disorder transition temperature can be estimated with knowledge of $\chi_{AB}N$ and f_A. The Flory−Huggins interaction parameter (χ_{AB}) between A and B segments becomes smaller when the penalty for mixing is reduced, which subsequently decreases the order−disorder transition temperature. In our case, the nontapered polymer showed a T_{ODT} of 282 °C, while the inverse-tapered material of nearly identical molecular weight and composition exhibited a T_{ODT} of 174 °C. Thus, it is clear that incorporating a relatively modest inverse taper (30 vol % of the overall polymer chain) can significantly increase block compatibility leading to a self-assembled double-gyroid network with similar shear modulus but

a substantially reduced melt processing temperature (108 °C lower for the inverse-tapered material). Additionally, though the molecular weight for the normal-tapered material is somewhat lower than that of the comparable nontapered copolymer, we can still conclude that normal tapering significantly influences block compatibility as expressed by a drop in T_{ODT}. In this case, we find that the difference in T_{ODT} between P(I−S)−OH and P(I−IS−S)−OH is 87 °C. A rough estimate of the effect of molecular weight on T_{ODT} allows us to postulate that ∼25 °C of the difference between the normal and nontapered materials can be ascribed to the change in molecular weight;[18] thus, the remainder of the difference (∼62 °C) is likely related to the incorporation of the taper. The greater drop in T_{ODT} from inverse-tapered P(I−SI−S)−OH to normal-tapered P(I−IS−S)−OH is attributable to long sequences of different chemistry (as opposed to the same chemistry in the case of normal-tapered materials) next to pure isoprene and styrene blocks, which leads to greater interfacial mixing.[18] These results indicate that we retain the ability to design materials that self-assemble into complex structures in narrow regions of the phase diagram, while exhibiting substantial and systematic control over thermodynamic interactions between blocks as measured by order−disorder transition temperatures. Although the present investigation does not calculate the interfacial thickness in tapered and nontapered block copolymers, it will be valuable to make a correlation between the polymer chain composition profile and the self-assembled material's interfacial thickness, interfacial composition profile, and the order−disorder transition temperature. These studies are currently in progress.

V. CONCLUSIONS

In this work we report the successful synthesis of tapered block copolymers that self-assemble into double-gyroid network structures with well-defined interfacial modifications between blocks, and we demonstrate the effect of normal and inverse tapering on the thermal transitions in our self-assembled materials. Synchrotron small-angle X-ray scattering and transmission electron microscopy analyses show that the incorporation of tapered regions up to 30% of the total copolymer volume does not extinguish the double-gyroid network. Subsequent thermal studies, through dynamic mechanical analysis, indicate that the normal and inverse tapered regions allow us to manipulate the order−disorder transition temperatures of our materials while retaining the desired network morphologies. We believe that these studies provide insight into methods for generating complex self-assembled structures that occur in relatively narrow regions of the phase diagram, while gaining greater systematic control over soft materials processability.

■ ASSOCIATED CONTENT

Ⓢ Supporting Information. GPC and ^{1}H NMR analysis for the tapered block copolymers as well as the complete DMA profiles for the nontapered P(I−S)−OH block copolymer. This material is available free of charge via the Internet at http://pubs.acs.org.

■ AUTHOR INFORMATION

Corresponding Author

*E-mail: thepps@udel.edu.

Author Contributions

†These authors contributed equally to this work.

■ ACKNOWLEDGMENT

This manuscript was prepared under cooperative agreement 70NANB7H6178 from NIST, U.S. Department of Commerce. The statements, findings, conclusions, and recommendations are those of the authors and do not necessarily reflect the view of NIST or the U.S. Department of Commerce. We gratefully acknowledge NSF-NER (CBET-0707507), NSF-CAREER (DMR-0645586), AFOSR-PECASE (FA9550-09-1-0706), and ACS PRF Grant (PRF-46864-67) for financial support. R. Roy acknowledges funding from NIH NCRR COBRE (NIH-2P20RR017716-06A1), and M. S. Tureau acknowledges an Air Products fellowship. We thank the W. M. Keck Electron Microscopy Facility for use of their TEM facilities. Portions of this work also were performed at the DuPont−Northwestern−Dow Collaborative Access Team (DND-CAT) located at Sector 5 of the Advanced Photon Source (APS). DND-CAT is supported by E.I. DuPont de Nemours & Co., The Dow Chemical Company, and the State of Illinois. Use of the APS was supported by the U.S. Department of Energy, Office of Science, Office of Basic Energy Sciences, under Contract DE-AC02-06CH11357. Use of the National Synchrotron Light Source, Brookhaven National Laboratory, was supported by the U.S. Department of Energy, Office of Science, Office of Basic Energy Sciences, under Contract DE-AC02-98CH10886. We acknowledge Dr. Lixia Rong for assistance in acquiring NSLS SAXS data.

■ REFERENCES

(1) Kim, H.-C.; Park, S.-M.; Hinsberg, W. D. *Chem. Rev.* **2010**, *110*, 146–177.
(2) Bates, F. S.; Schulz, M. F.; Khandpur, A. K.; Förster, S.; Rosedale, J. H.; Almdal, K.; Mortensen, K. *Faraday Discuss.* **1994**, *98*, 7–18.
(3) Bates, F. S.; Fredrickson, G. H. *Annu. Rev. Phys. Chem.* **1990**, *41*, 525–557.
(4) Khandpur, A. K.; Förster, S.; Bates, F. S.; Hamley, I. W.; Ryan, A. J.; Bras, W.; Almdal, K.; Mortensen, K. *Macromolecules* **1995**, *28*, 8796–8806.
(5) Förster, S.; Khandpur, A. K.; Zhao, J.; Bates, F. S.; Hamley, I. W.; Ryan, A. J.; Bras, W. *Macromolecules* **1994**, *27*, 6922–6935.
(6) Hajduk, D. A.; Harper, P. E.; Gruner, S. M.; Honeker, C. C.; Kim, G.; Thomas, E. L.; Fetters, L. J. *Macromolecules* **1994**, *27*, 4063–4075.
(7) Epps, T. H.; Cochran, E. W.; Bailey, T. S.; Waletzko, R. S.; Hardy, C. M.; Bates, F. S. *Macromolecules* **2004**, *37*, 8325–8341.
(8) Meuler, A. J.; Hillmyer, M. A.; Bates, F. S. *Macromolecules* **2009**, *42*, 7221–7250.
(9) Potschke, P.; Paul, D. R. *J. Macromol. Sci., Polym. Rev.* **2003**, *C43*, 87–141.
(10) Crossland, E. J. W.; Kamperman, M.; Nedelcu, M.; Ducati, C.; Wiesner, U.; Smilgies, D.-M.; Toombes, G. E. S.; Hillmyer, M. A.; Ludwigs, S.; Steiner, U.; Snaith, H. J. *Nano Lett.* **2009**, *9*, 2807–2812.
(11) Darling, S. B. *Energy Environ. Sci.* **2009**, *2* (12), 1266–1273.
(12) Hasegawa, H.; Hashimoto, T.; Hyde, S. T. *Polymer* **1996**, *37*, 3825–3833.
(13) Zielinski, J. M.; Spontak, R. J. *Macromolecules* **1992**, *25* (22), 5957–5964.
(14) Tsukahara, Y.; Nakamura, N.; Hashimoto, T.; Kawai, H. *Polym. J.* **1980**, *12*, 455–466.
(15) Hashimoto, T.; Tsukahara, Y.; Kawai, H. *Polym. J.* **1983**, *15*, 699–711.
(16) Pakula, T.; Matyjaszewski, K. *Macromol. Theory Simul.* **1996**, *5*, 987–1006.

(17) Hodrokoukes, P.; Floudas, G.; Pispas, S.; Hadjichristidis, N. *Macromolecules* **2001**, *34*, 650–657.
(18) Singh, N.; Tureau, M. S.; Epps, T. H. *Soft Matter* **2009**, *5*, 4757–4762.
(19) Mok, M. M.; Kim, J.; Wong, C. L. H.; Marrou, S. R.; Woo, D. J.; Dettmer, C. M.; Nguyen, S. T.; Ellison, C. J.; Shull, K. R.; Torkelson, J. M. *Macromolecules* **2009**, *42*, 7863–7876.
(20) Mok, M. M.; Kim, J.; Torkelson, J. M. *J. Polym. Sci., Part B: Polym. Phys.* **2008**, *46*, 48–58.
(21) Jiang, R.; Jin, Q.; Li, B.; Ding, D.; Wickham, R. A.; Shi, A.-C. *Macromolecules* **2008**, *41*, 5457–5465.
(22) Shull, K. R. *Macromolecules* **2002**, *35*, 8631–8639.
(23) Hodrokoukes, P.; Pispas, S.; Hadjichristidis, N. *Macromolecules* **2002**, *35*, 834–840.
(24) Samseth, J.; Spontak, R. J.; Smith, S. D.; Ashraf, A.; Mortensen, K. *J. Phys. IV* **1993**, *3*, 59–62.
(25) Mahajan, S.; Renker, S.; Simon, P. F. W.; Gutmann, J. S.; Jain, A.; Gruner, S. M.; Fetters, L. J.; Coates, G. W.; Wiesner, U. *Macromol. Chem. Phys.* **2003**, *204*, 1047–1055.
(26) Acar, M. H.; Matyjaszewski, K. *Macromol. Chem. Phys.* **1999**, *200*, 1094–1100.
(27) Epps, T. H.; Chatterjee, J.; Bates, F. S. *Macromolecules* **2005**, *38*, 8775–8784.
(28) Fetters, L. J.; Lohse, D. J.; Richter, D.; Witten, T. A.; Zirkel, A. *Macromolecules* **1994**, *27*, 4639–4647.
(29) Tureau, M. S.; Rong, L.; Hsiao, B.; Epps, T. H., III. *Macromolecules* **2010**, *43* (21), 9039–9048.
(30) Luzzati, V.; Spegt, P. A. *Nature* **1967**, *215*, 701–704.
(31) Vigild, M. E.; Almdal, K.; Mortensen, K. *Macromolecules* **1998**, *31*, 5702–5716.
(32) Shefelbine, T. A.; Vigild, M. E.; Matsen, M. W.; Hajduk, D. A.; Hillmyer, M. A.; Cussler, E. L.; Bates, F. S. *J. Am. Chem. Soc.* **1999**, *121*, 8457–8465.
(33) Bailey, T. S.; Pham, H. D.; Bates, F. S. *Macromolecules* **2001**, *34*, 6994–7008.
(34) We expect that the order−disorder transition temperature of the nontapered material will be slightly affected by the PI homopolymer content; however, this will not significantly influence our results.
(35) Lee, K. M.; Han, C. D. *Macromolecules* **2002**, *35*, 760–769.
(36) Kim, J. K.; Kim, M. I.; Kim, H. J.; Lee, D. H. *Macromolecules* **2007**, *40*, 7590–7593.